Pergamon

1359-4311(95)00089-5

Applied Thermal Engineering Vol. 16, No. 10, pp. 817–827, 1996

1359-4311/96 $15.00 + 0.00

ANALYSIS OF EVAPORATION OF NON-AZEOTROPIC REFRIGERANTS IN A HORIZONTAL TUBE

Chung-biau Chiou,* Ding-chong Lu† and Chi-chuan Wang†‡

†Department of Mechanical Engineering, National Chiao Tung University, Hsinchu 300, Taiwan and
‡Energy & Resources Laboratories, Industrial Technology Research Institute, Hsinchu 310, Taiwan

(*Received* 29 *November* 1995)

Abstract—Based on the two-phase separated model, a detailed one-dimensional model for binary mixtures had been proposed to study the in-tube evaporation in a horizontal tube. The present model can predict the detailed variation of the composition, temperature, heat transfer rate and pressure drop of various binary mixtures under constant heat flux, counter-flow, or parallel-flow conditions. The predicted results agree favorably with the Takamatsu *et al.* [*Int. J. Heat Mass Transfer* **36**, 3555–3563 (1993)] and Jung *et al.* [*Exp. Heat Transfer* **2**, 237–255 (1989)] experimental data. Also, it is found that the full evaporation of the non-azeotropic refrigerants may require a corresponding temperature higher than the saturation temperature of the less volatile component. The non-linear variation of the property plays an important role in the heat transfer and pressure drop characteristics of the refrigerant mixtures. Copyright © 1996 Elsevier Science Ltd.

Keywords—Non-azeotropic refrigerants, evaporation, model.

NOMENCLATURE

Cp	specific heat at constant pressure, kJ/kg.°C
D_i	inner diameter of the shell tube, m
D_{oh}	shell-side hydraulic diameter, m
d_i	tube-side inner diameter, m
d_h	tube-side hydraulic diameter, m
d_o	tube-side outer diameter, m
dA	local area, m²
dP	pressure drop, Pa
dZ	local tube length, m
E	parameter
F	parameter
f	friction factor
Fr	Froude number
G	mass flux, kg/m².s
g	gravity acceleration, m/s²
H	parameter
h	heat transfer coefficient, W/m².°C
i	enthalpy, J/kg
J	diffusion mass flux, kg/m².s
k	thermal conductivity, W/m.°C
L	parameter
Le	Lewis number (mass diffusivity/thermal diffusivity)
M	mass flow rate, kg/s
Q	heat flow rate, W
q	heat flux, W/m²
Pr	Prandtl number
p	pressure
$p_{\text{critical pressure}}$	critical pressure, bar
P_r	reduced pressure, $p/p_{\text{critical pressure}}$
Re	Reynolds number
S	parameter
T	temperature, °C
We	Weber number
X	liquid phase mass fraction of volatile component
Xf	flow quality (vapor mass flow rate/total mass flow rate)
Xt	thermodynamic quality
Y	vapor phase mass fraction of volatile component
Z	length in the axial direction, m

‡Author to whom correspondence should be addressed.

Greek letters

α	void fraction
β	mass transfer coefficient, m/s
δ	liquid film thickness, m
ϕ_{fo}	two-phase multiplier
μ	viscosity, Pa-s
ρ	density, kg/m^3
σ	surface tension, N/m

Subscripts

a	annulus
b	bulk
f	fluid
h	heating water
i	interface
in	inlet
l	liquid
m	mass
out	outlet
s	sensible
v	vapor
w	wall
wi	inner wall
wo	outer wall

INTRODUCTION

There is increased effort on research and development of advanced technology for the efficient use of energy, including waste heat recovery from various industrial processes with moderate and/or low temperatures. Accordingly, the increasing attention given to heat pump systems reflects this demand, since these systems are able to take energy from a lower temperature source. Therefore, non-azeotropic binary mixtures become attractive to the research for advanced vapor-compression systems. The thermodynamic cycle of the non-azeotropic mixture in a vapor-compression refrigeration system is called the Lorenz cycle [1]. There are several advantages in using the non-azeotropic mixture as a working fluid in refrigerating cycles and heat pumps. The merit of the Lorenz cycle is that the compression work load of the compressor and the thermodynamic irreversibilities in the evaporator and condenser can be reduced theoretically due to less temperature difference between the system and the environment. Besides, there is an important merit in the development of CFC/HCFC alternatives due to their smaller or zero ozone-depletion potential.

During the past decade, experimental efforts on horizontal flow boiling of refrigerant mixtures have been carried out extensively, and some correlations for the heat transfer coefficients have been proposed. A number of studies concerned with pool boiling, forced convective boiling and falling film evaporation of mixtures have been reported, as compiled in recent review articles by Wang and Chato [2] and Celata *et al.* [3]. However, the design tool of an evaporator model for the mixtures is not yet well established. As is well known, in the design of evaporation equipment for liquid mixtures, thermodynamic equilibrium is usually assumed. However, this is an approximation since temperature and concentration differences change during the evaporation process. Therefore, there will be a corresponding rise in the boiling point. This will result in the loss of superheat and eventually the available surface area may become insufficient to accomplish the heat duty. Consequently, the objective of this study is to develop a prediction method to evaluate the composition shift, pressure drop and heat transfer rate of binary refrigerant mixtures during the evaporation process.

ANALYSIS

The physical model and its detailed coordinate system are illustrated in Fig. 1. Actually, it is a double-pipe configuration, refrigerant vapor flows in the inner tube, while coolant flows in the annulus. The outer surface is insulated. Inside the tube, the flow geometry of the flow is assumed

annular with liquid film around the periphery of the tube and a continuous gas flow in the core. The vapor and liquid phases have differing velocities which are assumed to be one-dimensional. In the evaporating region, thermodynamic quasi-equilibrium exists at the vapor–liquid interface.

Interface equations

The differential control volume of the present model is also shown in Fig. 1. Since the mass fraction of the light component in the bulk vapor is greater than that at the interface, a counter-diffusion flux (J_v) of the light component occurs between the bulk vapor stream and the vapor–liquid interface. Similarly, a co-current diffusion flux (J_l) of the light component diffuses from the bulk liquid film to the vapor–liquid interface. The mass flux balance of the light component at the interface is obtained as follows:

$$\dot{M}_i X_i + J_l dA = \dot{M}_i Y_i - J_v dA, \tag{1}$$

where

$$J_l = \rho_l \beta_l (X_b - X_i) \tag{2}$$

$$J_v = \rho_v \beta_v (Y_b - Y_i)\,. \tag{3}$$

The counter-diffusion flux and the co-current diffusion flux result in a decrease and increase of evaporative mass flow rate at the interface, respectively. The liquid-phase mass transfer coefficient (β_l) is assumed to have a constant value of 0.0003 m/s, as suggested by Thome [4]. The vapor-phase mass transfer coefficient (β_v) is obtained from the Reynold analogy, as proposed by Lu and Lee [5], and is given by

$$\beta_v = \frac{h_v}{\rho_v C p_v}\,\mathrm{Le}^{2/3}\,. \tag{4}$$

The Gnielinski [6] correlation is adopted to obtain the vapor core heat transfer coefficient, namely,

$$h_v = \frac{k_v}{d_h}\,\frac{f_i/2(\mathrm{Re}_v - 1000)\mathrm{Pr}_v}{1.0 + 12.7(f_i/2)^{0.5}(\mathrm{Pr}_v^{2/3} - 1)}\,, \tag{5}$$

where the interfacial friction factor, f_i, is a function of the local void fraction and density ratio

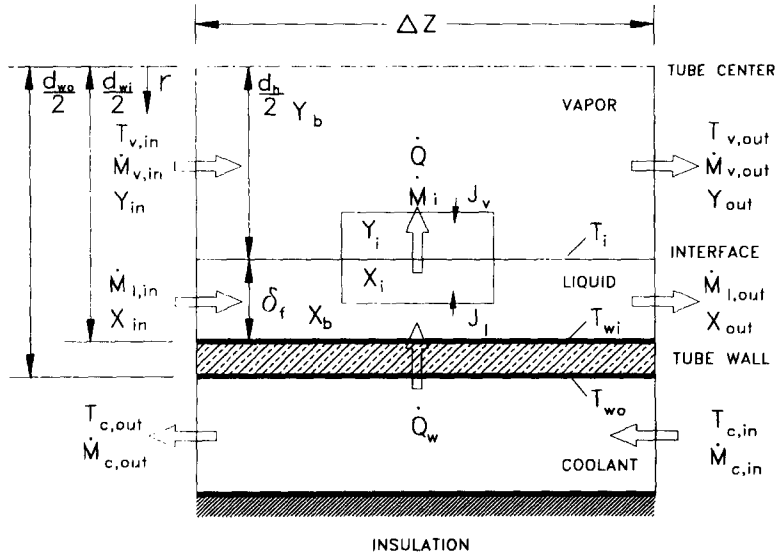

Fig. 1. Control volume diagram.

proposed by Whalley and Hewitt [7] as

$$f_i = f_0\left[1 + 12\left(\frac{\rho_l}{\rho_v}\right)^{1/3}(1-\alpha^{0.5})\right], \tag{6}$$

where the Fanning friction factor is obtained from

$$f_0 = 0.079\mathrm{Re}_v^{-0.25} \tag{7}$$

and the void fraction, α, is a function of the flow quality and density ratio, and is given by Chisholm [8] as

$$\alpha = \left[1 + \frac{1-Xf}{Xf}\left(\frac{\rho_v}{\rho_l}\right)^{0.5}\right]^{-1}. \tag{8}$$

Liquid film equations

The mass balance equation of the liquid film:

$$\dot{M}_{l,out} + \dot{M}_i = \dot{M}_{l,in}\,. \tag{9}$$

The mass balance equation of the light component:

$$\dot{M}_{l,in}X_{in} = \dot{M}_i Y_i + \dot{M}_{l,out}X_{out}\,. \tag{10}$$

Energy equation of the liquid film:

$$\dot{Q}_w = h_f(T_{wi} - T_i)dA\,. \tag{11}$$

The Liu and Winterton [9] correlation is used to evaluate the heat transfer coefficient of the liquid film near the wall, i.e.

$$h_f^2 = (Fh_l)^2 + (Sh_{pool})^2\,, \tag{12}$$

where

$$h_l = 0.023\left(\frac{k_l}{d_h}\right)\mathrm{Re}_l^0\mathrm{Pr}_l^{0.4} \tag{13}$$

$$h_{pool} = 55P_r^{0.12}q^{2/3}(-\log_{10}P_r)^{-0.55} \tag{14}$$

$$F = \left[1 + Xf\mathrm{Pr}_l\left(\frac{\rho_l}{\rho_v} - 1\right)\right]^{0.35} \tag{15}$$

$$S = (1 + 0.55F^{0.1}\mathrm{Re}_l^{0.16})^{-1}\,. \tag{16}$$

Vapor core equations

Mass balance equations of the bulk vapor core:

$$\dot{M}_{v,in} + \dot{M}_i = \dot{M}_{v,out}\,. \tag{17}$$

Mass balance equations of the light component:

$$\dot{M}_{v,in}Y_{in} + \dot{M}_l Y_i = \dot{M}_{v,out}Y_{out}\,. \tag{18}$$

Energy equation of the vapor core:

$$\dot{M}_{v,in}i_{in} + \dot{Q} = \dot{M}_{v,out}i_{v,out}\,, \tag{19}$$

where Q is the heat transfer rate through the interface, including latent heat transfer and sensible heat transfer, namely,

$$\dot{Q} = \dot{Q}_l + \dot{Q}_s\,, \tag{20}$$

where

$$\dot{Q}_l = \dot{M}_i i_{fg} \tag{21}$$

$$\dot{Q}_s = h_v[T_i - 0.5(T_{v,in} + T_{v,out})]dA \tag{22}$$

and the sensible heat transfer rate can also be expressed as

$$\dot{Q}_s = \dot{M}_{v,out} Cp_{v,out} T_{v,out} - \dot{M}_{v,in} Cp_{v,in} T_{v,in} . \tag{23}$$

Heating water and wall conduction equations

The energy equation of heating water is

$$\dot{Q}_w = \dot{M}_h Cp_h (T_{h,in} - T_{h,out}) \tag{24}$$

and the heat transfer rate can also be expressed as

$$\dot{Q}_w = h_a[0.5(T_{h,in} + T_{h,out} - T_{wo})] , \tag{25}$$

where h_a is the annulus heat transfer coefficient, and is determined by McMillen and Larson [10] as

$$h_a = 0.023 \frac{k_h}{D_h} \mathrm{Re}_h^{0.8} \mathrm{Pr}_h^{0.4} \left(\frac{D_i}{d_o} \right)^{0.45} . \tag{26}$$

The wall conduction equation is written by

$$\dot{Q}_w = 2\pi k_w \frac{T_{wo} - T_{wi}}{\ln\left(\frac{d_o}{d_i} \right)} dZ . \tag{27}$$

Pressure drop equations

The separated model is used to calculate the pressure drops of each control volume which was shown by Collier and Thome [11] as

$$-\frac{dP}{dZ} = \left[\frac{2f_l G^2}{d_i \rho_l} \right] \phi_{fo}^2 + G^2 \frac{d}{dZ} \left[\frac{Xf^2}{\alpha \rho_v} + \frac{(1 - Xf)^2}{(1 - \alpha)\rho_l} \right], \tag{28}$$

where the two-phase multiplier, ϕ_{fo}^2, is adopted from the Friedel correlation [12].

$$\phi_{fo}^2 = E + \frac{3.23LH}{\mathrm{Fr}^{0.045} \mathrm{We}^{0.035}} , \tag{29}$$

where

$$E = (1 - Xf)^2 + Xf^2 \frac{P_f f_v}{\rho_v f_l} \tag{30}$$

$$L = Xf^{0.78}(1 - Xf)^{0.224} \tag{31}$$

$$H + \left(\frac{\rho_l}{\rho_v} \right)^{0.91} \left(\frac{\mu_v}{\mu_l} \right)^{0.19} \left(1 - \frac{\mu_v}{\mu_l} \right)^{0.7} \tag{32}$$

$$\mathrm{Fr} = \frac{G^2}{g d_i \rho_h^2} \tag{33}$$

$$\mathrm{We} = \frac{G^2 d_i}{\rho_h \sigma} \tag{34}$$

$$\rho_h = \frac{\rho_v \rho_l}{\rho_l Xf + (1 - Xf)\rho_v} \tag{35}$$

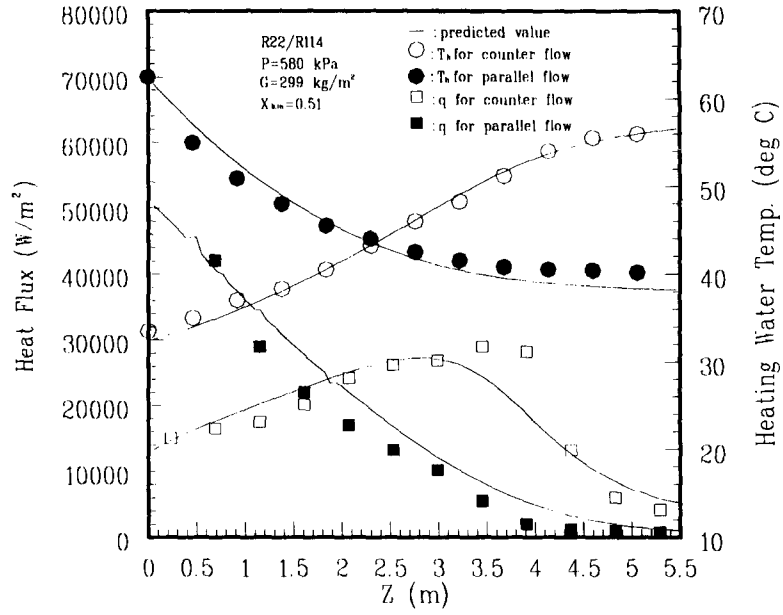

Fig. 2. Comparison of heating water temperature (T_h) and heat flux (q) between the present model and Takamatsu's [15] experimental data.

$$f_v = 0.046\mathrm{Re}_v^{0.2} \tag{36}$$

$$f_l = 0.079\mathrm{Re}_l^{0.25} . \tag{37}$$

The thermodynamic and transport properties of the mixtures were evaluated using a computer program [13].

RESULTS AND DISCUSSION

Figure 2 presents the experimental data of Takamatsu [14] for the mixture of 51 wt% R22/49 wt% R114. The axial distributions of the annulus temperature T_h and the heat flux q with both counter-flow and parallel-flow conditions are shown in this figure. As expected, the heating water temperatures increase with the axial location for the counter-flow configuration and decrease with the axial location for the parallel-flow configuration. The heat flux decreases with the axial location for the parallel-flow configuration, and the heat flux for the counter-flow configuration first increases with the axial location, and reaches a maximum value near $Z = 3.7$ m and levels off very quickly as Z increases further. On close examination of the experimental data, one can find that the thermodynamic quality of the refrigerant is approximately equal to unity at this position. The thermodynamic quality is given as

$$Xt = \frac{X_{b,in} - X_i}{Y_i - X_i} , \tag{38}$$

where $X_{b,in}$ is the inlet mass fraction of the light component evaluated at the bulk of the liquid phase of the mixture, X_i and Y_i are the local compositions of liquid and vapor phase at the interface, respectively. Accordingly, since the thermodynamic quality is close to unity, the level-off phenomenon of the heat flux is due to the dry-out of the refrigerant. Also shown in the figure are the predictions by the present model. As seen, the predicted results agree well with those of the experimental data for both parallel- and counter-flow conditions.

Figure 3 shows the predicted values of bulk concentration of vapor and liquid versus flow quality for various binary mixtures. The mixtures include R22/R114, R22/R124 and R32/R134a. Table 1 shows the comparison of the thermodynamic and transport properties of the pure refrigerants and their mixtures at two concentrations, namely 0.5 and 0.1. All the thermodynamic and transport properties are evaluated using a computer program (NIST REFPROP 4.01) at the reduced pressure

of 0.15. The reduced pressure is defined as $p/p_{\text{critical pressure}}$. As seen in Fig. 3, at $P_r = 0.15$, $X_{b,in} = 0.5$, $q = 20\ \text{kW/m}^2$, $G = 300\ \text{kg/m}^2$, and under the counter-flow conditions, the bulk composition of the light component decreases along the axial location. In particular, the R22/R114 mixtures reveal a sharp decrease as compared to other mixtures. The reason for this phenomenon can be explained from the phase diagram of the mixtures as depicted in Fig. 4. The lower line in the phase diagram, the bubble point line, represents the variation of the liquid saturation temperature with composition. The dew point line represents the variation of the saturated vapor temperature with composition. The area between the dew point and the bubble point represents the temperature glide, and can be loosely identified as the degradation potential of a particular mixture. As seen in Fig. 4, the temperature glide of the R22/R114 mixture of the phase diagram is much larger than those for R22/R124 and R32/R134a mixtures. This indicates that the more volatile component of the R22/R114 mixture, R22, is evaporated more rapidly than in other mixtures. Therefore, a much sharper decrease of bulk composition for R22/R114 mixture is expected.

The phase diagram of Fig. 4 also indicates that, when the evaporation proceeds, X_i decreases along the tube and eventually an increase of vapor temperature is found. On further heating to a temperature corresponding to the dew point, all the liquid is vaporized to give a vapor of the same composition as the original liquid. The last drop of the liquid to disappear is very rich in the less volatile composition. For an initial given $X_{b,in} = 0.5$, the concentration of the last drop of the depleted liquid is approximately equal to 0.19 for the R22/R114 mixture, as depicted in the phase diagram. However, the present calculation shows that the X_i is less than 0.1 for the R22/R114 mixture when the axial location Z is greater than 3 m. In fact, the concentration of the R22/R114 mixture is considerably lower than 0.19. The present calculations suggest that the in-tube evaporation of the non-azeotropic refrigerants is a non-equilibrium process. In fact, Kedzierski *et al.* [15] suggest that the liquid–vapor interface may be the only portion which is possibly in thermodynamic equilibrium. The smaller concentration and its corresponding pressure will result in an increase of saturation temperature. In an addition, there is a further drop in composition from the bulk of the liquid to the vapor interface, and this may result in an additional increase of the saturation temperature. Eventually, to have completely depleted the liquid refrigerants, it

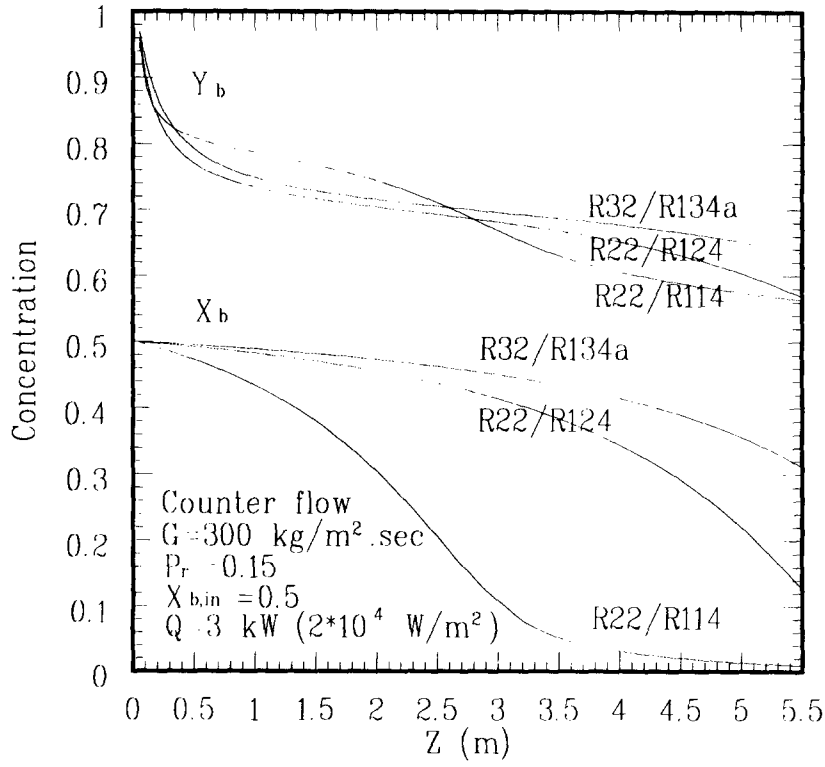

Fig. 3. Predicted vapor (Y_b) and liquid (X_b) bulk compositions for various binary mixtures.

Table 1. Thermodynamic properties of five pure refrigerants and their mixtures

	X	M (kg/kmole)	i_{fg} (kJ/kg)	k_l (mW/m².K)	k_v (mW/m².K)	μ_l (μPa·s)	μ_v (μPa·s)	Cp_l (kJ/kg.K)	Cp_v (kJ/kg.K)	ρ_l (kg/m³)	ρ_v (kg/m³)	$\frac{K_l^{0.6}}{(Cp_l/\mu_l)^{0.4}}$
R22	–	86.48	122.76	95.50	10.30	209.7	20.9	1.177	0.705	1255.9	26.3	122.80
R32	–	52.02	207.03	152.89	12.20	162.5	11.6	1.676	0.895	1062.5	19.2	127.43
R114	–	170.94	110.08	51.78	12.90	236.0	13.5	1.069	0.794	1328.6	45.5	92.48
R124	–	136.47	136.03	62.35	13.20	215.9	13.1	1.173	0.827	1288.6	39.9	96.14
R134a	–	102.03	178.35	78.68	14.00	207.4	12.6	1.426	0.943	1190.9	35.4	100.60
R22/R114	0.5	128.71	169.60	81.24	11.07	261.2	13.0	1.090	0.741	1335.8	32.2	125.21
R22/R124	0.5	111.48	175.20	81.63	11.29	226.9	12.8	1.152	0.763	1295.8	32.0	116.09
R32/R134a	0.5	77.03	265.70	122.10	12.22	192.6	12.1	1.516	0.908	1153.5	24.6	124.05
R22/R114	0.1	162.49	132.20	60.24	12.35	269.1	13.4	1.055	0.781	1366.3	41.7	107.3
R22/R124	0.1	131.47	146.70	66.88	12.67	224.6	13.0	1.157	0.813	1300.9	37.9	102.42
R32/R134a	0.1	97.03	199.50	88.69	13.37	210.6	12.5	1.431	0.933	1197.0	32.4	108.6

is likely that the corresponding temperature of the non-azeotropic refrigerants is higher than the saturation temperature of the less volatile component. The experimental measurements of the in-tube condensation from Kornota and Stocker [16] and the corresponding theoretical results from Lu and Lee [17] had suggested that the temperature corresponding to complete condensation of non-azeotropic refrigerants must be lower than the saturation of the pure light component at the end of condensation. Alternatively, it is likely that the liquid near the fully evaporated state of non-azeotropic refrigerants may require a corresponding temperature higher than the saturation temperature of the less volatile component.

Additional evidence for the incompleteness of the dry-out phenomenon of the mixtures may be due to the difference in flow pattern between pure and mixed refrigerant. An investigation of the flow pattern for the mixtures of R402a and R404a was carried out by Kattan *et al.* [18]. They observed that the flow patterns of the mixtures are generally not the same as those of pure refrigerants. Kattan *et al.* [18] found that the flow pattern of the mixtures with a stratified regime is often encountered even though their liquid Froude numbers were 13 and 16 times above the

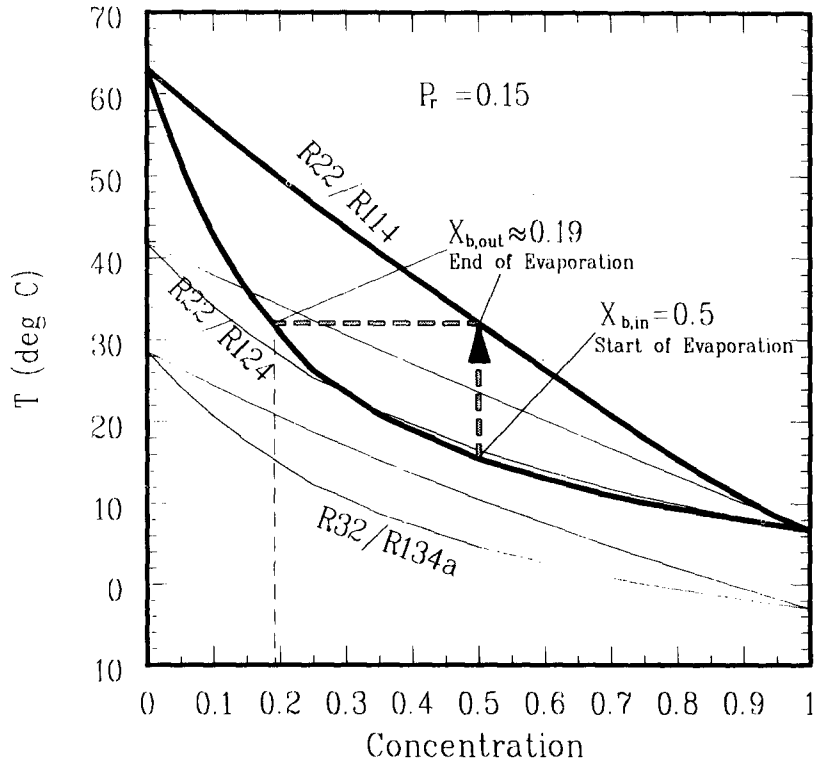

Fig. 4. Phase diagram of various binary mixtures.

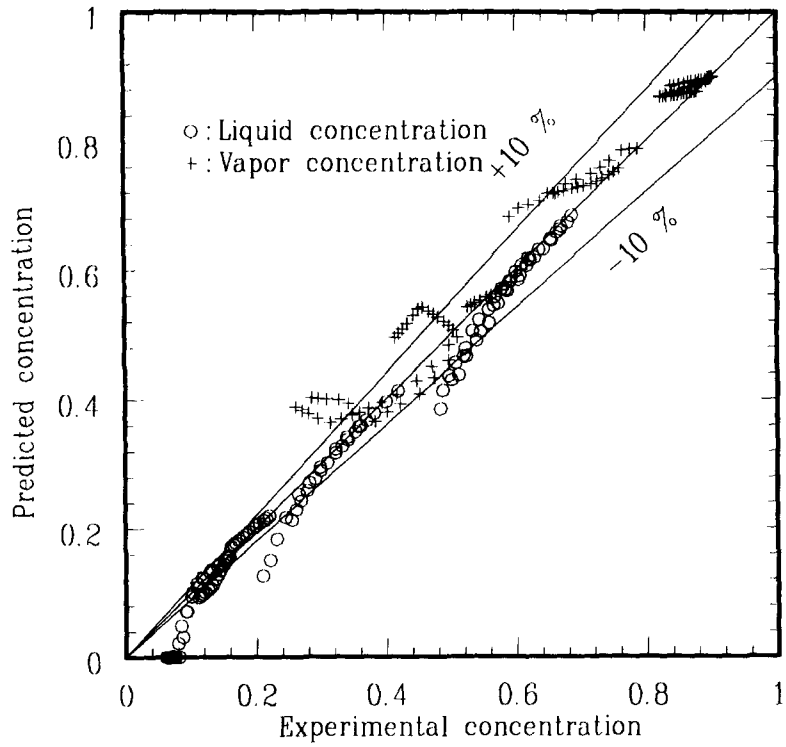

Fig. 5. Comparison of vapor and liquid compositions between the present model and Jung's [21] experimental data.

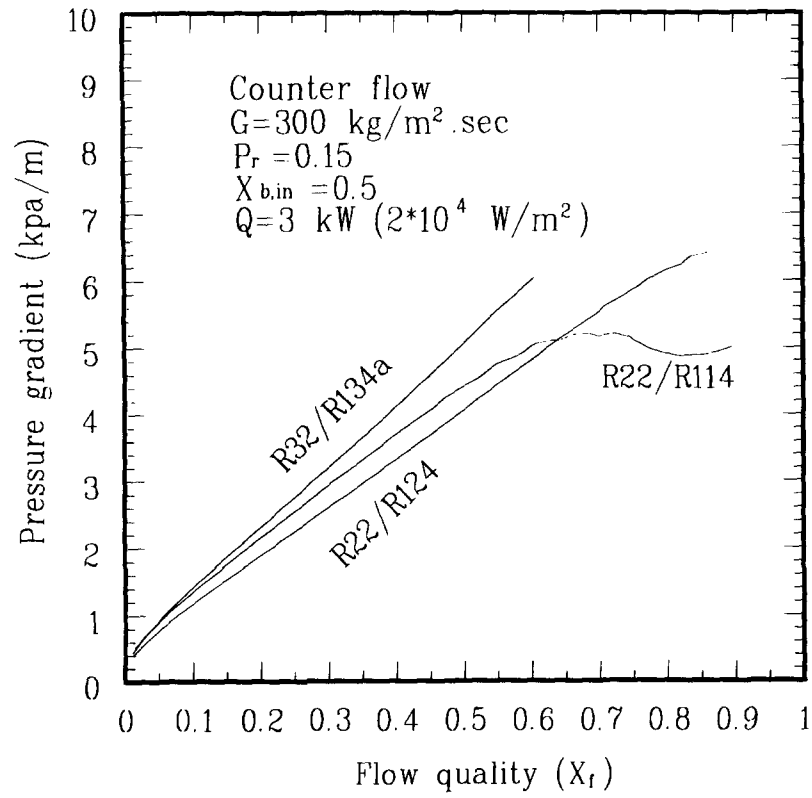

Fig. 6. Predicted pressure gradients for various binary mixtures.

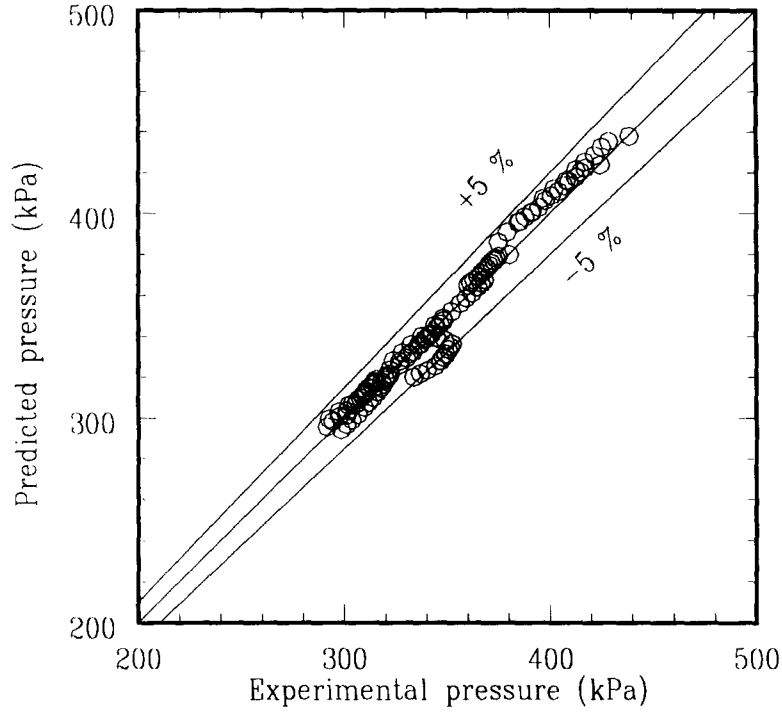

Fig. 7. Comparison of pressure variations inside the horizontal tube between the present model and Jung's [21] experimental data.

recommended values of 0.04 and 0.05, as suggested by Shah [19] and Kandikar [20] for pure refrigerants. This suggests a delay of the dry-out phenomenon for the mixture refrigerant.

Figure 5 presents the comparisons of the predicted concentration with the experimental data measured by Jung *et al.* [21]. As seen, good agreements with the measured data are reported for both vapor and liquid concentration.

Figure 6 shows the predicted pressure gradient versus flow quality for various binary mixtures. The pressure gradient for the mixtures increases with flow quality. However, the R22/R114 mixture reveals a level-off phenomenon when flow quality is greater than 0.7. The reason for the level off is due to the non-linear variation of the property. On close examination of the calculated results, we find that the density ratio, ρ_l/ρ_v, plays an important role in the calculation of pressure drop. Actually, ρ_l/ρ_v changes from 41.5 to 31.3 for the R114/R22 mixture, from 40.5 to 37.9 for the R22/R124 mixture, and from 47 to 49.5 for the R32/R134a mixture. As indicated from equations (28)–(37), the two-phase multiplier is related to $(\rho_l/\rho_v)^{0.91}$. As a result, the pressure gradient for the R22/R114 mixture reveals a level-off phenomenon for the higher-quality region, since a considerable reduction of ρ_l/ρ_v is found compared to other mixtures. Note that the pure refrigerants generally do not exhibit such a phenomenon, since no significant variation of the properties for the pure refrigerant is reported. Figure 7 presents the comparison of the evaporation pressure variation inside the horizontal tube between the predictions and Jung *et al.*'s [15] data. As seen, all the predicted pressure variations inside the test tube fall within a deviation of $\pm$ 5%. This result reveals that the present model can successfully predict the variation of evaporation pressure of the refrigerant mixtures.

CONCLUSION

A one-dimensional model is proposed to evaluate the heat transfer and pressure drop characteristics of mixtures. Some important results in the present investigation are summarized as follows:

1. The present model can predict the detailed variation of the composition, temperature and pressure drop of non-azeotropic refrigerants.

2. It is likely that the liquid near the fully evaporated state of the non-azeotropic refrigerants may require a corresponding temperature higher than the saturation temperature of the less volatile component.

3. The level-off phenomenon of the pressure drop of the R22/R114 mixture is mainly due to the change of density ratio and is more pronounced than those of R22/R124 and R32/R134a mixtures. This suggests that the non-linear variation of the properties of the mixtures plays an important role in the heat and momentum transfer of the mixtures.

Acknowledgements—This work was supported by the National Science Council of R.O.C. under grant NSC 84-2212-E-009-001.

REFERENCES

1. A. Lorenz and K. Meutzner, On application of non-azeotropic two component refrigerants in domestic refrigerators and home freezers. *XIV Int. Congress of Refrigeration*, Moscow, IIR, Paris, paper BZ 43 (1975).
2. S. P. Wang and J. C. Chato, Review of recent research on heat transfer with mixtures. Part 2: boiling and evaporation. Paper presented at ASHRAE winter meeting, paper number CH-95-23-3 (1995).
3. G. P. Celata, M. Cumo and T. Setaro, A review of pool and forced convective boiling of binary mixtures. *Exp. Thermal Fluid Science* **9**, 367–381 (1994).
4. J. R. Thome, Two-phase heat transfer to new refrigerants. 10*th Int. Heat Transfer Conf.*, Vol. 1, pp. 19–41 (1994).
5. D. C. Lu. and C. C. Lee, An analytical model of condensation heat transfer of non-azeotropic refrigerant mixtures in a horizontal tube.. *ASHRAE Trans.* **100**(2), 721–731 (1994).
6. V. Gnielinski, New equations for heat and mass transfer in turbulent pipe and channel flow. *Int. Chem. Engng* **16**, 359–368 (1976).
7. P. B. Whalley and G. F. Hewitt, The correlation of liquid entrainment fraction and entrainment rate in annular two-phase flow. Report AERE-R9187, UK AEA, Harwell, UK (1978).
8. D. Chisholm, *Two-phase Flow in Pipelines and Heat Exchangers*, Chapter 4. George Godwin, London (1983).
9. Z. Liu and R. H. S. Winterton, A general correlation for saturated and subcooled flow boiling in tubes and annuli, based on a nucleate pool boiling equation. *Int. J. Heat Mass Transfer* **34**(11), 2759–2766 (1991).
10. E. L. McMillen and R. E. Larson, Discussion on annular heat transfer coefficients for turbulent flow.. *American Institute of Chemical Engineers* **40**(2), 147–153 (1950).
11. J. G. Collier and J. R. Thome, *Convective Boiling and Condensation*, 3rd Edition, Chapter 2. Oxford University Press, Oxford (1994).
12. L. Friedel, Improved friction pressure drop correlations for horizontal and vertical two-phase pipe flow. *Proc. European Two-phase Flow Group Meeting*, Paper E2, Ispra, Italy (1979).
13. NIST, REFPROP. National Institute of Standards and Technology, Gaithersburg, MD (1994).
14. H. S. Takamatsu and T. Fujii, A correlation for forced convective boiling heat transfer of non-azeotropic refrigerant mixture of HCFC22/CFC114 in a horizontal smooth tube. *Int. J. Heat Mass Transfer* **36**(14), 3555–3563 (1993).
15. A. Kedzierski, J. H. Kim and D. A. Didion, Cause of the apparent heat transfer degradation for refrigerant mixtures. *Two-phase Flow and Heat Transfer, ASME HTD* **197**, 149–158 (1992).
16. E. Kornota and W. M. Stoecker, Flow regimes of refrigerant mixtures condensing inside tubes. ORNL/Sub/81-7762/4&01, Oak Ridge National Laboratory, Tennessee (1985).
17. D. C. Lu and C. C. Lee, Investigation of condensation heat transfer of non-azeotopic refrigerant mixtures in a horizontal tube, 10*th International Heat Transfer Conf.*, CD14 (1994).
18. N. Kattan, J. R. Thome and D. Favrat, R502 and two near-azeotropic alternatives. Part II: two-phase flow patterns. ASHRAE Transactions, paper presented at Winter Meeting, CH-95-14-3 (3879) (1995).
19. M. M. Shah, Chart correlation for saturated boiling heat transfer: equations and further study. *ASHRAE Trans.* **88**(1), 185–196 (1982).
20. S. G. Kandikar, A general correlation for saturated two-phase flow boiling heat transfer inside horizontal and vertical tubes. *J. Heat Transfer* **112**, 219–228 (1990).
21. D. S. Jung, M. McLinden and R. Radermacher, Measurement technique for horizontal flow boiling heat transfer with pure and mixed refrigerants. *Exp. Heat Transfer* **2**, 237–255 (1989).